

A LOW VOLTAGE MICROMACHINED OPTICAL SWITCH BY STRESS-INDUCED BENDING

Richard T. Chen[†], Hung Nguyen, Ming C. Wu

Tel: (310) 825-6859, Email: wu@ee.ucla.edu

Department of Electrical Engineering, University of California at Los Angeles
66-147D Engineering IV Building, Los Angeles, CA 90095-1594

[†]Lucas Varsity Novasensor, 1055 Mission Court, Fremont, CA 94539

ABSTRACT

In this paper, a novel electrostatically actuated 2x2 fiber optic switch with very low operating voltage is presented. Using stress-induced bending of polysilicon plates, a vertical mirror is raised above the substrate. Electrostatic force is used to attract the mirror to the substrate to switch between the cross and the parallel states of the optical switch. The stress-induced curvature of the polysilicon beam substantially lowers the operating voltage of the switch. Large mirror displacement (300 μm) and low operating voltage (20 V) are achieved simultaneously. Sub-millisecond switching time (<600 μsec) and reliable operation (>14 million cycles) have been demonstrated. The insertion loss is measured to be 0.55 dB and 0.7 dB for single mode fibers in the cross and parallel states, respectively.

INTRODUCTION

Interest in optical switching has been increasing due to the rapid growth of the information super highway. Optomechanical switches are preferred in many applications because of their low insertion loss and crosstalk. They are also wavelength and polarization independent. Conventional optomechanical switches are, however, bulky, slow, expensive, and unreliable. The Micro-Electro-Mechanical Systems (MEMS) technology has become a viable technology for implementing optomechanical switches. The size and weight are greatly reduced in micromechanical switches. In addition, they are inherently fast and have low power consumption. The batch fabrication process can also lower the cost of the switches. More importantly, MEMS technology allows large matrix switches to be monolithically integrated on a single chip.

Though many MEMS optical switches have been reported using both bulk and surface micromachining techniques [1-4], most of them have high operating voltage or small mirror displacement. Low voltage switches with large mirror displacement are needed for the matrix switch applications. Low operating voltage enables the switch to be directly driven by standard CMOS integrated circuits. Large mirror displacement is essential for switches with collimated optical beams. In this paper, we report on a novel MEMS fiber optic switch with low operating voltage and large mirror

displacement. The switch is fabricated using a standard surface-micromachining technique, and can potentially be mass-produced at a very low cost. 2x2 optical switches with operating voltage of 20 V, switching time of 600 μsec , and optical insertion loss of 0.7 dB for single mode fibers have been achieved.

PRINCIPLE AND DESIGN

To achieve low operating voltage, a curved electrostatic actuator is used for switching. The switch consists of a gold-coated hinged micro-mirror (300 x 175 μm^2) attached to the end of a polysilicon cantilever beam. The cantilever is coated with a stressed layer of Cr and Au on its top surface. As the structure is released, the stress in the metal film causes the cantilever beam to curve upward. The switch is in the cross (transmission) state when the mirror is

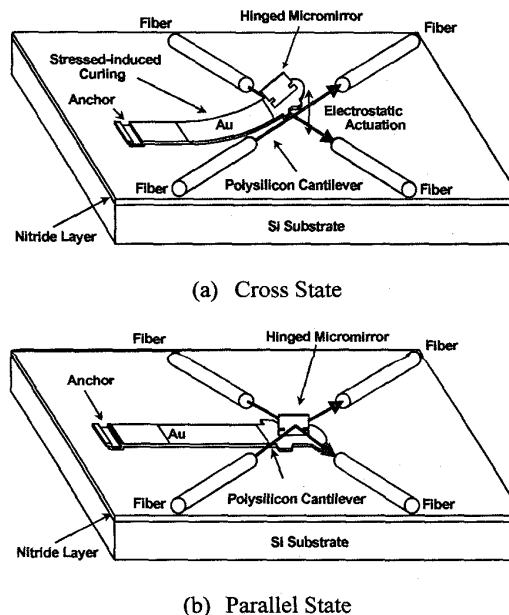


Figure 1. Schematic of the low-voltage MEMS fiber optic switch realized by stress-induced bending of polysilicon cantilever beam.

raised above the light paths. A voltage is applied between the curved polysilicon beam and the substrate to operate the switch. The beam is electrostatically attracted to the substrate changing it from the cross state to the parallel (reflection) state, as shown in Fig. 1. The curvature of the beam creates a zipping actuation [5] that reduces the voltage needed for the mirror to snap-down. A similar actuator using Cr/Al has been reported in [6].

Proper cantilever design is needed to obtain the desired beam deflection. Methods for designing stress induced curved cantilever beams have been studied in Ref. [6-9]. The cantilever becomes curved from a bending moment caused by the variation in stress between the polysilicon and metal films. The electrode bends upward because the polysilicon has a compressive residual stress while the Cr/Au film has a tensile residual stress. The curvature of the cantilever and the maximum beam deflection are determined by its physical dimensions and material properties. The dimensions are labeled in Fig. 2.

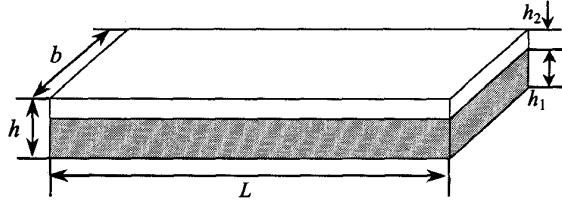


Figure 2. Dimensions of the cantilever beam.

When two films of different residual stresses share an interface at equilibrium, the induced forces, P_1 and P_2 , and the moments, M_1 and M_2 , must balance [10]:

$$\begin{aligned} P_1 &= P_2 = P \\ P \cdot \frac{h}{2} &= M_1 + M_2 = M \end{aligned} \quad (1)$$

where h is the total thickness of the beam. Using an equivalent beam strength [7],

$$(E \cdot I)_{equiv} = \frac{E_2 \cdot b \cdot h_2^3}{12(1+m \cdot n)} \cdot K, \quad (2)$$

where $K = 1 + 4m \cdot n + 6m \cdot n^2 + 4m \cdot n^3 + m^2 \cdot n^2$,

$$m = \frac{E_1}{E_2} \quad \text{and} \quad n = \frac{h_1}{h_2}, \quad (3)$$

where E_1 and E_2 are the Young's modulus and h_1 and h_2 are the thicknesses for the polysilicon and the metal films, respectively. The relationship between the stress-induced internal force, P , and the radius of curvature, ρ , can be determined:

$$P = \frac{2 \cdot (E \cdot I)_{equiv}}{h \cdot \rho}. \quad (4)$$

Since both films share an interface, the strain for each material can be equated:

$$\frac{\sigma_1}{E_1} + \frac{P}{E_1 \cdot h_1 \cdot b} + \frac{h_1}{2 \cdot \rho} = \frac{\sigma_2}{E_2} - \frac{P}{E_2 \cdot h_2 \cdot b} - \frac{h_2}{2 \cdot \rho} \quad (5)$$

where the first term is due to residual stresses, σ_1 and σ_2 , the second is from the axial force, P , and the last is from the beam curvature, ρ . Solving for the radius of curvature from Eqs. (2), (4), and (5) gives

$$\frac{1}{\rho} = \frac{6(m \cdot \sigma_2 - \sigma_1)}{h \cdot E_2 (3m + K[n(1+n)^2]^{-1})}. \quad (6)$$

The maximum displacement, δ , of the tip of the beam is

$$\delta = \rho \left(1 - \cos\left(\frac{L}{\rho}\right) \right), \quad (7)$$

which can be calculated through geometry. Therefore, using Equations (6) and (7), the desired height for the optical fiber switch can be achieved by varying the length or the thickness of the cantilever beam.

To determine the resonant frequency of the switch, the equation for a singly clamped cantilever beam is used [11]:

$$f_R = \frac{1}{2\pi} \sqrt{\frac{k}{m}} = \frac{1.03}{2\pi} \cdot \frac{t \cdot v}{L^2}, \quad (8)$$

where $v = \sqrt{\frac{E}{\rho_D}}$ = longitudinal acoustic velocity,

- k = beam spring constant,
- m = beam mass,
- t = beam thickness,
- L = beam length,
- E = Young's modulus of beam material,
- ρ_D = density of beam material.

To maximize the resonant frequency and reduce the switching time, the length should be as short as possible.

FABRICATION

The fiber optic switch is fabricated using the Multi-User MEMS Processes (MUMPs) available through the MEMS Technology Application Center at North Carolina (MCNC). This process uses an isolation layer of nitride, three structural layers of polysilicon (poly), and sacrificial layers of phosphosilicon glass (PSG). Hydrofluoric (HF) acid is used to release the structures. The switch consists of a $300 \times 175 \mu\text{m}^2$ gold-coated micro-mirror mounted on the end of a cantilever beam using micro-hinges [12]. Micro-latches are used to lock the micro-mirror in the vertical position. The entire length of the cantilever beam is 1.5 mm. The polysilicon beam is $1.5 \mu\text{m}$ thick. A 20-nm-thick Cr film and a $0.5\text{-}\mu\text{m}$ -thick Au film are deposited on the surface of the polysilicon to induce the bending. The length of the curved section of the beam is $730 \mu\text{m}$. A scanning electron

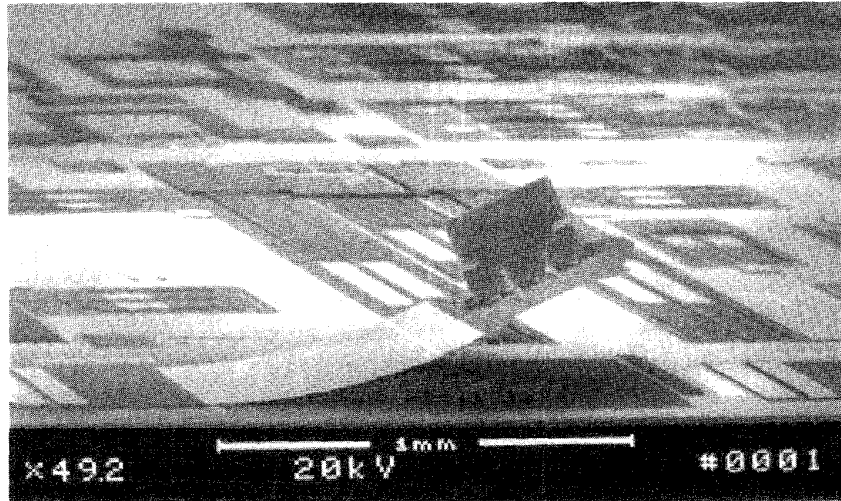


Figure 3. SEM micrograph of switch.

micrograph (SEM) of the optical switch is shown in Fig 3.

The Cr/Au layer is also used for the mirror surface. A curved mirror surface will distort the reflection from the mirror, causing a higher insertion loss. The mirror is fabricated using a sandwiched layer of PSG in between two layers of polysilicon. This three-layer structure has a total thickness of $4.25\ \mu\text{m}$ for rigidity to prevent any curving caused by the metal layer. The PSG is completely sealed by the polysilicon layers, which protects it from the sacrificial HF acid etch. A cross-section of the mirror is shown in Fig. 4.

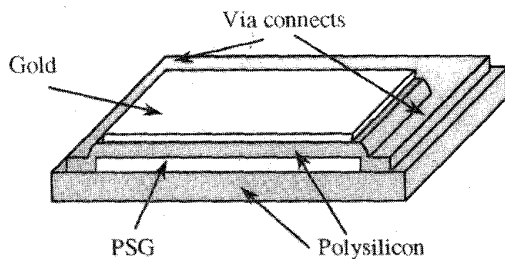


Figure 4. Cross-section of micro-mirror.

During operation, a voltage is applied to the cantilever beam, attracting it to the grounded substrate. A $0.5\text{-}\mu\text{m}$ -thick nitride layer insulates the switch from the substrate. To prevent damage to the micro-hinges during operation, a polysilicon plate is inserted underneath the mirror end of the cantilever, which restricts electrostatic force and contact to only the curved section of the beam. A schematic drawing of the end of the cantilever beam is shown in Fig. 5. The polysilicon stopper causes the straight section of the cantilever under the mirror to tilt upward. The height of the cantilever tip is about $40\ \mu\text{m}$ above the substrate when the cantilever snaps down.

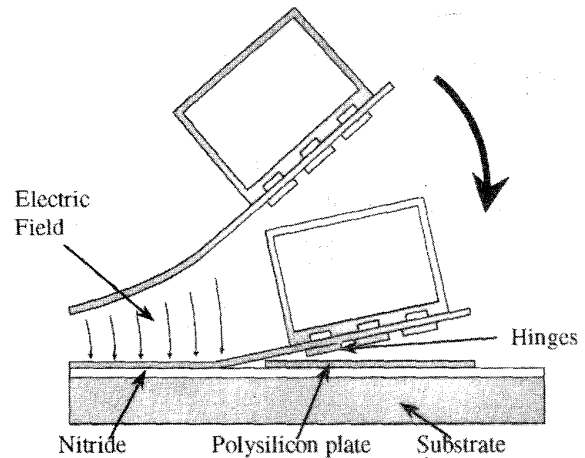


Figure 5. Schematic of micro-mirror during operation.

MEASUREMENTS AND RESULTS

The deflection angle of the cantilever beam was measured using a HeNe laser. Relative angle changes were recorded from the reflection of the laser at the tip of the cantilever beam. The beam deflection as a function of applied voltage is plotted in Fig. 6. The snap-down voltage was $20\ \text{V}$ and the release voltage was $16\ \text{V}$.

The frequency response of the switch was measured using a stroboscope. The switch was biased by a sinusoidal wave with voltages between 0 and $17\ \text{V}$. Figure 7 shows displacement of the cantilever tip versus the driving frequency. A measured resonant frequency was $1\ \text{KHz}$. The experimental value of the resonant frequency matches very well with the $1.006\ \text{KHz}$ obtained from Eq. (8).

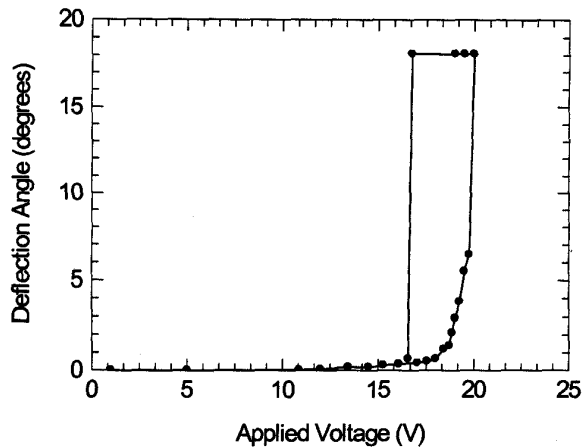


Figure 6. Deflection angle of cantilever beam versus applied voltage.

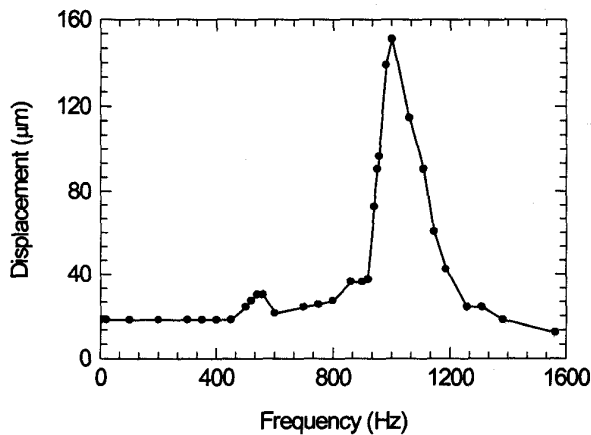


Figure 7. The frequency response of the switch.

The switch was designed for a maximum deflection of 400 μm at the tip of the cantilever beam. Cantilever beams of lengths 800-1600 μm were fabricated to determine the residual stress in the metal film. Figure 8 shows measured maximum deflection heights for different length beams.

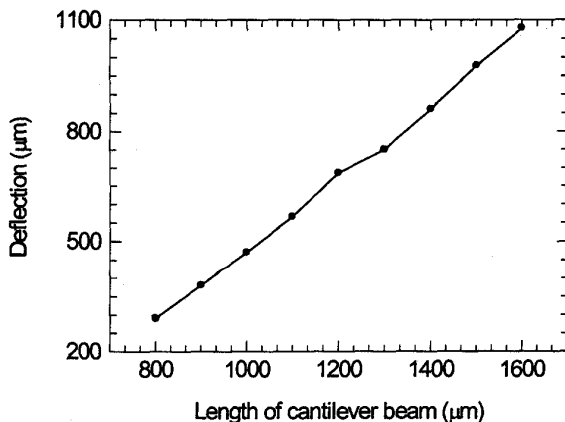
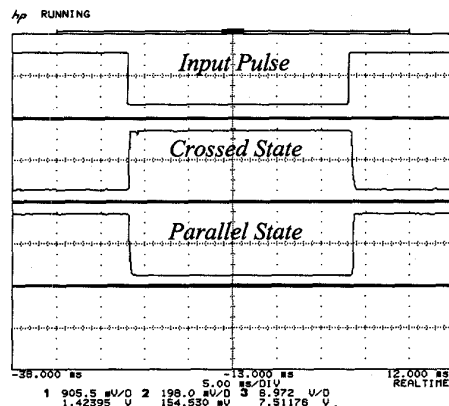


Figure 8. Maximum deflection versus beam length.

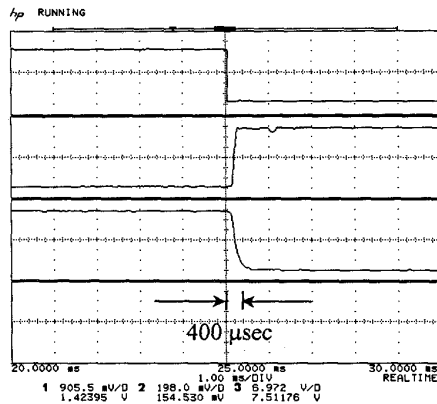
For the theoretical calculation, the value for the residual stress in the polysilicon was assumed to be -450 MPa [13], which is typical for deposited polysilicon. The residual stress in thin films varies greatly with thickness, deposition temperature, doping levels, and other fabrication parameters. Assuming a value for polysilicon is sufficient to obtain a relative stress value for the metal film so that the length for a desired deflection height can be determined. Using Eqs. (6) and (7), the relative residual stress value for the metal film was found to be 73 MPa. To obtain a 400 μm deflection, the required length for the curved section of the beam was 730 μm , taking into account the 500- μm -long straight section under the mirror. The actual beam height was 346 μm . The difference from the theoretical value can be attributed to the variance in the fabrication process. The actual maximum displacement of the mirror was 306 μm .

The performance of the switch was measured using a tunable semiconductor laser with a wavelength of 1550 nm. The optical beam is expanded from a single mode fiber and collimated by a ball lens. The diameter of the collimated beam ($\sim 50 \mu\text{m}$) is much smaller than the size of the mirror, which ensures complete coverage of the optical beam. The optical insertion loss for single mode fibers was measured to be 0.55 dB in the cross state (collimator to collimator) and 0.7 dB in the parallel state. The switch had negligible crosstalk ($< -80 \text{ dB}$) between both states. These measurements include the loss of one additional fiber connector. Curved mirrors that were not fabricated using the poly/PSG/poly stack had an insertion loss of 2.7 dB. To understand the cause of the excess insertion loss in the parallel state, we measured the total optical power of the input collimated beam and the reflected beam in free space. Over 98% of the optical power is reflected by the mirror and less than 2.0% of light is transmitted through the mirror.

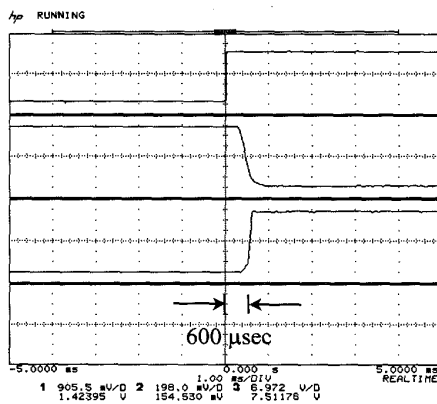
The dynamic response of the switch was measured using a HP834440D photodetector. The switch was driven by a square wave with a 20 Hz repetition frequency. The dynamic response of the switch is shown in Fig. 9. The fall time, corresponding to snap-down of the switch, was 600 μsec . The rise time, corresponding to release of the switch, was 400 μsec .



(a) 20 Hz Input Pulse



(b) Rise time (1 msec/div)



(c) Fall time (1 msec/div)

Figure 9. The dynamic response of the switch.

We have also conducted a cycling test of the switch. The switch was operated for over 14 million cycles. No operational degradation of the switch was observed. The edge of the beam near anchor to the substrate, which is the highest stress point in the cantilever beam, did not fail. The hinges were not damaged and the mirror remained vertical.

CONCLUSION

We have reported a novel silicon surface-micromachined 2x2 optical fiber switch for telecommunication applications. A stress-induced curved actuator was integrated with a vertical micro-mirror to demonstrate a low-voltage (20 V) and large-mirror-displacement (300 μm) optical switch. The switching times were 400 μsec and 600 μsec for the rise and the fall times, respectively. The insertion losses for single mode fibers were 0.55 dB for the cross state and 0.7 dB for the parallel state.

ACKNOWLEDGEMENTS

The authors would like to thank Li Fan for helpful discussions, Thomas Jung for help with the optical measurements, and John Su for taking the SEM pictures. This project was supported in part by DARPA.

REFERENCES

- [1] M. Mita, D. Miyauchi, H. Toshiyoshi and H. Fujita, "An Out-of-Plane Polysilicon Actuator with a Smooth Vertical Mirror for Optical Switch Applications," *IEEE LEOS Summer Topical Meetings*, pp. 33-34, 1998.
- [2] C. Marxer, M.-A. Gretillat, N.F. de Rooij, R. Battig, O. Anthamatten, B. Valk, and P. Vogel, "Vertical Mirrors Fabricated by Reactive Ion Etching for Fiber Optical Switching Applications," *IEEE The Tenth Annual International Workshop on Micro Electro Mechanical Systems*, pp. 49-54, 1997.
- [3] S.S. Lee, L. S. Huang, C. J. Kim, M. C. Wu, "2x2 MEMS Fiber Optic Switches with Silicon Sub-Mount For Low-Cost Packaging," *Solid-State Sensor and Actuator Workshop Hilton Head Island*, pp. 281-284, 1998.
- [4] V. Aksyuk, B. Barber, C. R. Giles, R. Ruel, L. Stulz and D. Bishop, "Low Insertion Loss Packaged and Fiber-Connectorized SI Surface-Micromachined Reflective Optical Switch," *Solid-State Sensor and Actuator Workshop Hilton Head Island*, pp. 79-82, 1998.
- [5] R. Legtenberg, E. Berenschot, M. Elwenspoek, and J. Fluitman, "Electrostatic Curved Electrode Actuators," *Proceedings IEEE Micro Electro Mechanical Systems 1995*, pp. 37-42, 1995.
- [6] T. Yasuda, I Shimoyama and H. Miura, "Cmos Drivable Electrostatic Microactuator with Large Deflection," *IEEE The Tenth Annual International Workshop on Micro Electro Mechanical Systems*, pp. 90-95, 1997.
- [7] M. W. Judy, Y.-H. Cho, R. T. Howe and A. P. Pisano, "Self-Adjusting Microstructures (SAMS)," *Proceedings IEEE Micro Electro Mechanical Systems 1991*, pp. 51-56, 1991.
- [8] C.-L. Tsai and A. K. Henning, "Out-of-plane microstructures using stress engineering of thin films," *Proceedings of the SPIE-The International Society for Optical Engineering*, pp. 124-32, 1995
- [9] J. Gorrell, "Thin film Metallization for Micro-Bimetallic Actuators," *Solid-State Sensor and Actuator Workshop Hilton Head Island*, pp. 300-303, 1998.
- [10] S. Timoshenko, *Strength of Materials*, Krieger, New York, 1976.
- [11] G. T. A. Kovacs, *Micromachined Transducers Sourcebook*, WCB/McGraw-Hill, New York, 1998.
- [12] K. S. J. Pister, M. W. Judy, S. R. Burgett, and R. S. Fearing, "Microfabricated hinges," *Sensors and Actuators A-Physical*, Vol. 33, no. 3, pp. 249, 1992.
- [13] R. T. Howe, *Polysilicon Films and Interfaces*, *Mat. Res. Soc. Symp. Proc.*, Vol 106, pp. 213-224, 1989.